Reorientation phase transitions in thin magnetic films: a review of the classical vector spin model within the mean-field approach

L. Udvardi†‡§, L. Szunyogh†‡, A. Vernes‡ and P. Weinberger‡

† Department of Theoretical Physics, Budapest University of Technology and Economics, Budafoki út 8, H-1521, Budapest, Hungary
‡ Center for Computational Materials Science, Technical University Vienna, Gumpendorferstrasse 1a, A-1060 Vienna, Austria

Abstract

The ground-state and the finite-temperature phase diagrams with respect to magnetic configurations are studied systematically for thin magnetic films in terms of a classical Heisenberg model including magnetic dipole–dipole interaction and uniaxial anisotropy. Simple relations are derived for the occurrence of the various phase boundaries between the different regions of the magnetic orientations. In particular, the range of the first- and second-order reorientation phase transitions are determined for bilayers and trilayers.

§1. Introduction

Recent developments of thin-film technologies enable the growth of ultrathin magnetic films deposited on non-magnetic substrates to be controlled. Because of their challenging application as high-storage magnetic recording media, much attention (Gradmann 1986, Allenspach *et al.* 1990, Pappas *et al.* 1990, 1992, Allenspach 1994, Li *et al.* 1994, Berger and Hopster 1996, Garreau *et al.* 1996, Farle *et al.* 1997, Gubiotti *et al.* 1997) has been devoted to the novel properties of these new structures. From a technological point of view, the study of the magnetic phase transitions and, in particular, of reorientations of the magnetization is playing a major role. In comparison with bulk systems, the presence of surfaces and interfaces leads to an enhancement of the magnetocrystalline anisotropy due to spin–orbit coupling. The magnetocrystalline anisotropy often prefers a magnetization perpendicular to the surface, while the magnetic dipole–dipole interaction and the entropy at finite temperatures favour an in-plane magnetization. Consequently, as observed in many Fe- or Co-based ultrathin films (Gradmann 1986, Allenspach *et al.* 1990, Pappas *et al.* 1990, 1992, Allenspach 1994, Li *et al.* 1994, Berger and Hopster 1996, Garreau *et al.* 1996), a reorientation from an out-of-plane to an in-plane direction of the magnetization occurs by increasing both the thickness of the film and the temperature. Relativistic first principles calculations using the local-spin-density approximation turned out to be sufficiently accurate to reproduce the critical thickness of the reorientation (Szunyogh *et al.* 1995, 1997b, Zabloudil *et al.* 1998).

§ Email: udvardi@phy.bme.hu

In the case of thin Ni films deposited on a Cu(001) surface, the opposite beha-
viour was revealed; the magnetization was found to be in plane for fewer than seven
Ni monolayers; however, it became perpendicular to the surface beyond this thick-
ness. Below the switching thickness near 0 K, even an increase in the temperature
induces a similar reversed reorientation (Farle *et al.* 1997, Gubiotti *et al.* 1997). The
main origin of the above reorientation was attributed to the fact that strain-induced
anisotropy of the inner layers prefers a perpendicular magnetization (Hjortstam *et
al.* 1997, Uiberacker *et al.* 1999).

Subsequent to the pioneering work of Mills (1989), who predicted the existence
of a canted non-collinear ground state for a semi-infinite ferromagnetic system, and
that of Pescia and Pokrovsky (1990) who, by using a renormalization group treat-
ment of a continuum vector field model, for the first time described the temperature
induced (normal) reorientation phase transition, a considerable number of theore-
tical attempts, mostly by means of different statistical spin models, were suggested in
order to explain the above findings for the thickness- and temperature-driven re-
orientation transitions. In some attempts, classical vector spin models were used
within the mean-field approximation (Taylor and Györffy 1993, Hucht and Usadel
1996, 1997, 1999a,b, 2000, Jensen and Bennemann 1998, Hu *et al.* 1999) or in terms
of Monte Carlo simulations (Taylor and Györffy 1993, Serena *et al.* 1993, Chui 1995,
Hucht *et al.* 1995, Hucht and Usadel 1996, MacIsaac *et al.* 1996). A quantum-spin
description of reorientation transitions has also been provided in terms of spin-wave
theory (Bruno 1991), mean-field theory (Moschel and Usadel 1994, 1995) and many-
body Green function techniques (Fröbrich *et al.* 2000a,b, Jensen *et al.* 2000), and by
using Schwinger bosonization (Timm and Jensen 2000). Although, the mean-field
theory is not expected to give a sufficiently accurate description of low-dimensional
systems, it turned out that it is a successful tool to study spin reorientation transi-
tions and yields qualitatively correct predictions (Moschel and Usadel 1994, 1995,
Hucht and Usadel 1997, 1999a,b, 2000, Jensen and Bennemann 1998, Hu *et al.*
1999). It also should be noted that an itinerant-electron Hubbard model revealed
the sensitivity of reorientation transitions with respect to electron correlation effects
(Herrmann *et al.* 1998).

For layered systems, the following simple model Hamiltonian can be used to
study reorientation transitions (for example Taylor and Györffy (1993)):

$$H = -\frac{1}{2} \sum_{(p,i),(q,j)}^{\mathrm{NN}} J\mathbf{s}_{pi} \cdot \mathbf{s}_{qj} - \sum_{p,i} \lambda_p (s_{pi}^z)^2$$

$$+ \frac{1}{2} \sum_{(p,i) \neq (q,j)} \omega \left(\frac{\mathbf{s}_{pi} \cdot \mathbf{s}_{qj}}{r_{pi,qj}^3} - 3 \frac{(\mathbf{s}_{pi} \cdot \mathbf{r}_{pi,qj})(\mathbf{s}_{qj} \cdot \mathbf{r}_{pi,qj})}{r_{pi,qj}^5} \right), \tag{1}$$

where $\mathbf{s}_{pi}(|\mathbf{s}_{pi}| = 1)$ is a classical vector spin at lattice position i in layer p and $\mathbf{r}_{pi,qj}$ is
a vector pointing from site (p,i) to site (q,j) measured in units of the two-dimen-
sional (2D) lattice constant a of the system. Although our previous calculations of
the Heisenberg exchange parameters in thin Fe, Co and Ni films on Cu(001) showed
some layer-dependence (Szunyogh and Udvardi 1998, 1999), in the first term of
equation (1) we only consider a uniform nearest-neighbour coupling parameter J
(as indicated by the superscript NN) throughout the film. Similarly, as we neglect the
well-known surface and interface-induced enhancement of the spin moments, we use
a single parameter $\omega = \mu_0 \mu^2 / 4\pi a^3$ (with μ_0 the magnetic permeability and μ an

average magnitude of the spin moments), characterizing the magnetic dipole–dipole interaction strength in the third term of equation (1). As revealed also by first-principles calculations (see Weinberger and Szunyogh (2000), and references therein), the uniaxial magnetocrystalline anisotropy depends very sensitively on the type of surface or interface, the layerwise resolution of which can vary from system to system. Therefore, the corresponding parameters λ_p in the second term of equation (1) remain layer dependent; the variety of these anisotropy parameters leads to rich magnetic phase diagrams covering the experimentally detected features mentioned above. For example, in a previous study (Udvardi *et al.* 1998) we pointed out that, even in the absence of a fourth-order anisotropy term, for a very asym-metric distribution of λ_p with respect to the layers, the Heisenberg model in equation (1) can yield a canted (non-collinear) ground state. This feature cannot be obtained within a phenomenological single-domain picture.

In the following, we first investigate the possible ground states of the Hamiltonian (1). Then we perform a systematic mean-field study of the different kinds of temperature-induced reorientation transition, devoting special attention to the case of bilayers and trilayers. Specifically, we define general conditions for the reversed reorientation. Most researchers in the past focused on proving the existence of different reorientations and detected only some parts of the phase diagram, where first- and second-order phase transitions occurred. Here, we describe the full range of uniaxial anisotropies λ_p, for which first- or second-order reorientation phase transi-tions can exist. Finally, we attempt to summarize the results and impacts of a mean-field approach.

§2. GROUND STATE

Confining ourselves to spin states in which the spins are parallel in a given layer, but their orientations may differ from layer to layer, that is

$$\mathbf{s}_{pi} = \mathbf{s}_p = (\sin(\theta_p)\cos(\phi_p), \sin(\theta_p)\sin(\phi_p), \cos(\theta_p)), \tag{2}$$

where θ_p and ϕ_p are the usual azimuthal and polar angles with the z axis normal to the planes, the energy of N layers per 2D unit cell can be written as

$$E_N(\theta_1, \theta_2, \ldots, \theta_N; \phi_1, \phi_2, \ldots, \phi_N) = -\frac{1}{2}\sum_{p,q=1}^{N}(Jn_{pq} - A_{pq}\omega)\cos(\theta_p)\cos(\theta_q)$$

$$-\frac{1}{2}\sum_{p,q=1}^{N}(Jn_{pq} + \frac{1}{2}A_{pq}\omega)\sin(\theta_p)\sin(\theta_q)$$

$$\times \cos(\phi_p - \phi_q) - \sum_{p=1}^{N}\lambda_p\cos^2(\theta_p), \tag{3}$$

with n_{pq} being the number of nearest neighbours in layer q of a site in layer p, and A_{pq} the magnetic dipole–dipole coupling constants (see the appendix in the paper by Szunyogh *et al.* (1995)):

$$\sum_{j}'\frac{1}{r_{p0,qj}^3}\left(I - 3\frac{\mathbf{r}_{p0,qj} \otimes \mathbf{r}_{p0,qj}}{r_{p0,qj}^2}\right) = A_{pq}\begin{pmatrix} -\frac{1}{2} & 0 & 0 \\ 0 & -\frac{1}{2} & 0 \\ 0 & 0 & 1 \end{pmatrix}, \tag{4}$$

Table 1.   Dipole–dipole coupling constants as defined in equation (4) for the surfaces of cubic structures.

Structure	A_{11}	A_{12}	A_{13}	A_{14}
Sc (100)	9.0336	−0.3275	−0.000 55	$< 10^{-5}$
Sc (111)	11.0342	5.9676	0.405 6	0.014 6
Bcc (100)	9.0336	4.1764	−0.327 46	0.012 38
Bcc (111)	11.0342	15.8147	5.967 6	−4.066 2
Fcc (100)	9.0336	1.4294	−0.022 6	0.000 26
Fcc (111)	11.0342	0.4056	0.001 13	$< 10^{-5}$

which is valid for square and hexagonal 2D lattices, such as the (100) and (111) surfaces of cubic systems (I is the three-dimensional (3D) unit matrix, while $\otimes$ stands for the tensorial product of two vectors). For 3D translational invariant underlying parent lattices (Weinberger 1997), A_{pq} depends only on $|p - q|$, that is the distance between layers p and q. In table 1 we summarize these constants for the first few layers of the most common cubic structures. As the magnetic dipole–dipole interaction is clearly dominated by the positive first-layer (and second-layer) couplings, for ferromagnetic systems ($J > 0$), a minimum of the energy in equation (3) corresponds to the case when all polar angles ϕ_p are identical. Therefore, the ϕ-dependence in equation (3) disappears and the expression

$$E_N(\boldsymbol{\theta}_1, \boldsymbol{\theta}_2, \ldots, \boldsymbol{\theta}_N) = -\frac{1}{2} \sum_{p,q=1}^{N} (Jn_{pq} - A_{pq}\omega) \cos(\boldsymbol{\theta}_p) \cos(\boldsymbol{\theta}_q)$$

$$-\frac{1}{2} \sum_{p,q=1}^{N} (Jn_{pq} + \tfrac{1}{2} A_{pq}\omega) \sin(\boldsymbol{\theta}_p) \sin(\boldsymbol{\theta}_q) - \sum_{p=1}^{N} \lambda_p \cos^2(\boldsymbol{\theta}_p), \quad (5)$$

has to be minimized with respect to θ_p. The corresponding Euler–Lagrange equations are then

$$\frac{\partial E_N(\boldsymbol{\theta}_1, \boldsymbol{\theta}_2, \ldots, \boldsymbol{\theta}_N)}{\partial \boldsymbol{\theta}_p} = \sum_{q=1}^{N} (Jn_{pq} - A_{pq}\omega) \sin(\boldsymbol{\theta}_p) \cos(\boldsymbol{\theta}_q)$$

$$- \sum_{q=1}^{N} (Jn_{pq} + \tfrac{1}{2} A_{pq}\omega) \cos(\boldsymbol{\theta}_p) \sin(\boldsymbol{\theta}_q)$$

$$+ 2\lambda_p \sin(\boldsymbol{\theta}_p) \cos(\boldsymbol{\theta}_p)$$

$$= 0. \quad (6)$$

Obviously, a uniform in-plane $\{\theta_p = \pi/2\}$ and a normal-to-plane $\{\theta_p = 0\}$ orientation satisfy equation (6). The energies of these two particular spin-states coincide if

$$\sum_{p=1}^{N} \frac{\lambda_p}{\omega} = \tfrac{3}{4} \sum_{p,q=1}^{N} A_{pq}, \quad (7)$$

which defines an $(N - 1)$-dimensional hyperplane in the N–dimensional space of parameters $\{\lambda_p/\omega\}$. If the magnetization changes continuously across this plane, in its vicinity there should exist solutions with canted magnetization. Moreover, the saddle points of the energy functional in equation (5),

$$\det \left| \frac{\partial E_N}{\partial \theta_p \partial \theta_q} \right|_{\{\theta_p = 0, \pi/2\}} = 0, \tag{8}$$

define the boundaries of the canted zone,

$$\det \left| \left[\sum_{r=1}^{N} \left(\frac{J}{\omega} n_{pr} + \frac{1}{2} A_{pr} \right) - 2 \frac{\lambda_p}{\omega} \right] \delta_{pq} - \left(\frac{J}{\omega} n_{pq} - A_{pq} \right) \right| = 0, \tag{9}$$

and

$$\det \left| \left[\sum_{r=1}^{N} \left(\frac{J}{\omega} n_{pr} - A_{pr} \right) + 2 \frac{\lambda_p}{\omega} \right] \delta_{pq} - \left(\frac{J}{\omega} n_{pq} + \frac{1}{2} A_{pq} \right) \right| = 0, \tag{10}$$

for the uniform in-plane and normal-to-plane magnetizations, respectively. For a bilayer we derived the explicit expressions of equations (9) and (10) (Udvardi *et al.* 1998).

In order to study the canted region, instead of solving the Euler–Lagrange equations (6) directly, we fixed a configuration $\theta_1^*, \theta_2^*, \ldots, \theta_N^*$ and determined $\lambda_1, \lambda_2, \ldots, \lambda_N$ by demanding that equation (6) must be satisfied, that is

$$\lambda_p = \frac{1}{2} \sum_{q=1}^{N} (Jn_{pq} + \frac{1}{2} A_{pq} \omega) \frac{\sin (\theta_q^*)}{\sin (\theta_q^*)} - \frac{1}{2} \sum_{q=1}^{N} (Jn_{pq} - A_{pq} \omega) \frac{\cos (\theta_q^*)}{\cos (\theta_p^*)}. \tag{11}$$

Substituting these parameters into equation (5), one easily can express the difference of the energies between the corresponding configurations as

$$E_N(\theta_1 = \theta_2 = \cdots = \theta_N = 0) - E_N(\theta_1^*, \theta_2^*, \ldots, \theta_N^*)$$

$$= \frac{1}{2} \sum_{pq}^{N} (n_{pq} J - A_{pq} \omega) \left(\frac{\cos (\theta_p^*)}{\cos (\theta_q^*)} + \frac{\cos (\theta_q^*)}{\cos (\theta_p^*)} - 2 \right) \tag{12}$$

and

$$E_N \left(\theta_1 = \theta_2 = \cdots = \theta_N = \frac{\pi}{2} \right) - E_N(\theta_1^*, \theta_2^*, \ldots, \theta_N^*)$$

$$= \frac{1}{2} \sum_{p,q}^{N} (n_{pq} J + \frac{1}{2} A_{pq} \omega) \left(\frac{\sin (\theta_p^*)}{\sin (\theta_q^*)} + \frac{\sin (\theta_q^*)}{\sin (\theta_p^*)} - 2 \right). \tag{13}$$

Note that the position of the minimum $\{\theta_p^*\}$ as well as the minimum energy $E_N(\{\theta_p^*\})$ are functions of the parameters J, ω and $\{\lambda_p\}$. Obviously, whenever the parameters fall into the region between the two hyperplanes defined by equations (9) and (10), the energy of non-collinear states is always below or equal to the energy of the collinear in-plane or normal-to-plane solutions.

We showed that, for a bilayer, $\lambda_1 = \lambda_2 = 3(A_{11} + A_{12})\omega/4$ implies a collinear ground state spin configuration (Udvardi *et al.* 1998). This state is, however, continuously degenerate, that is the energy is independent of the orientation of the magnetization. Such a critical point in the phase diagram also exists for multilayers ($N \geqslant 3$). That is, from equations (12) and (13) it follows that for $\theta_1^* = \theta_2^* = \cdots = \theta_N^* = \theta^*$, $E_N(\{\theta_p^*\})$ is independent of θ^*. In terms of equation (11), the corresponding point in the parameter space $\{\lambda_p/\omega\}$ is given by

$$\frac{\lambda_p}{\omega} = \tfrac{3}{4} \sum_{q=1}^{N} A_{pq}. \tag{14}$$

Evidently, the hyperplanes given by equations (9) and (10) touch the hyperplane, separating the in-plane and normal-to-plane regions (equation (7)), at the point defined by equation (14). It is worthwhile to mention that this is the only point where canted collinear solutions can exist. This critical point was also found by Hucht and Usadel (1996) for a monolayer, but they did not prove its existence for multilayers.

§ 3. FINITE TEMPERATURE

Introducing the coupling constants

$$c_{pq}^{x} = n_{pq}J + \tfrac{1}{2}\omega A_{pq}, \qquad c_{pq}^{z} = n_{pq}J - \omega A_{pq}, \tag{15}$$

the molecular field corresponding to the Hamiltonian (1) at layer p can be written as

$$H^p(\theta, \phi) = -\sum_{q=1}^{N} c_{pq}^{x}[m_p^x \sin(\theta)\cos(\phi) + m_p^y \sin(\theta)\sin(\phi)]$$

$$- \sum_{q=1}^{N} c_{pq}^{z} m_q^z \cos(\theta) - \lambda_p \cos^2(\theta), \tag{16}$$

where $m_p^\alpha = \langle s_p^\alpha \rangle$ ($\alpha = x, y, z$). Similar to the ground state (see § 2), because of the in-plane rotational symmetry of the above effective Hamiltonian, the in-plane projections of all the average magnetic moments $\mathbf{m}_p$ are aligned. Therefore, by choosing an appropriate coordinate system, m_p^y can be taken to be zero in equation (16). The partition function is then defined by

$$Z = \prod_{p=1}^{N} Z_p, \tag{17}$$

$$Z_p = 2\pi \int_{-\pi/2}^{\pi/2} \exp\{\beta[b_p^z \cos(\theta) + \lambda_p \cos^2(\theta)]\} J_0[-\mathrm{i}\beta b_p^x \sin(\theta)] \sin(\theta)\, \mathrm{d}\theta, \tag{18}$$

where

$$b_p^{x(z)} = \sum_{q=1}^{N} c_{pq}^{x(z)} m_q^{x(z)}, \tag{19}$$

$\beta = 1/k_\mathrm{B} T$, k_B is the Boltzmann constant and T is the temperature. The minimization of the free-energy with respect to the average magnetizations leads to the following set of nonlinear equations

$$m_p^x = \frac{2\mathrm{i}\pi}{Z_p} \int_{-\pi/2}^{\pi/2} \sin(\theta)\exp\{\beta[b_p^z \cos(\theta) + \lambda_p \cos^2(\theta)]\} J_1[-\mathrm{i}\beta b_p^x \sin(\theta)]\sin(\theta)\, \mathrm{d}\theta$$

$$\tag{20}$$

and

$$m_p^z = \frac{2\pi}{Z_p} \int_{-\pi/2}^{\pi/2} \cos(\theta) \exp\{\beta[b_p^z \cos(\theta) + \lambda_p \cos^2(\theta)]\} J_0[-i\beta b_p^x \sin(\theta)] \sin(\theta) \, d\theta.$$

(21)

In equations (17), (20) and (21), J_0 and J_1 denote Bessel functions of zero and first order respectively (Abramowitz and Stegun 1972).

By using a high-temperature expansion, equations (20) and (21) become decoupled (see appendix A). Consequently, the magnetization can go to zero either via an in-plane or via a normal-to-plane direction at temperatures T_x and T_z respectively, and the higher of these temperatures can be associated with the Curie temperature T_C. Clearly, an out-of-plane to in-plane reorientation phase transition can occur only when the ground-state magnetization is out of plane and $T_z < T_x = T_C$. In the case of a reversed reorientation transition, the ground state magnetization has to be in-plane (or canted) and $T_x < T_z = T_C$.

Expanding T_x and T_z up to first order in the anisotropy parameters λ_p, leads to the following expressions (see appendix A):

$$T_x = \frac{1}{3k_B}\left[n_{11}J + \tfrac{1}{2}A_{11}\omega + 2(n_{12}J + \tfrac{1}{2}A_{12}\omega)\cos\left(\frac{\pi}{N+1}\right)\right]$$
$$-\frac{4}{15(N+1)}\sum_{p=1}^{N}\lambda_p \sin^2\left(\frac{p\pi}{N+1}\right),$$

(22)

and

$$T_z = \frac{1}{3k_B}\left[n_{11}J - A_{11}\omega + 2(n_{12}J - A_{12}\omega)\cos\left(\frac{\pi}{N+1}\right)\right]$$
$$+\frac{8}{15(N+1)}\sum_{p=1}^{N}\lambda_p \sin^2\left(\frac{p\pi}{N+1}\right).$$

(23)

The above expressions imply that, if the anisotropy parameters λ_p are small, T_x is larger than T_z. As the anisotropy parameters are increasing, the difference between T_z and T_x decreases. The two temperatures coincide, if the following condition is fulfilled:

$$\sum_{p=1}^{N}\frac{\lambda_p}{\omega}\sin^2\left(\frac{p\pi}{N+1}\right) = \frac{5(N+1)}{8}\left[A_{11} + 2A_{12}\cos\left(\frac{\pi}{N+1}\right)\right].$$

(24)

Above the hyperplane determined by equation (24), that is for $T_x < T_z$, the uniaxial anisotropy is large enough to keep the magnetization normal to the surface as long as the temperature reaches T_C.

First-principles calculations on $(\mathrm{Fe, Co, Ni})/\mathrm{Cu}(001)$ overlayers revealed (Újfalussy *et al.* 1996, Szunyogh *et al.* 1997a, Szunyogh and Udvardi 1998, 1999, Uiberacker *et al.* 1999), that the uniaxial magnetic anisotropy energy and the magnetic dipole–dipole interaction are two to three orders of magnitude smaller than the exchange coupling. Thus, for physically relevant parameters, the boundaries of the canted ground state fixed by equations (9) and (10) are close to the hyperplane defined by equation (7). Apart from this tiny range of canted ground states, tem-

perature-induced out-of-plane to in-plane reorientation can occur in the parameter space $\{\lambda_p/\omega\}$ between the two hyperplanes given by equations (7) and (24). It is worthwhile to mention that the positions of these hyperplanes are determined only by the magnetic dipole–dipole constants A_{pq}.

An example for an out-of-plane to in-plane reorientation transition in a film five layers thick is shown in figure 1. Neglecting the fourth-order anisotropy terms, the parameters of the system have been chosen to be identical with those characteristic to a Co$_5$/Au(111) overlayer (Udvardi *et al.* 1998). Because of the highly asymmetric distribution of λ_p with respect to the layers, the system has a non-collinear canted ground state. As the temperature increases, the magnetization in each layer turns into the plane of the film. The system keeps its non-collinear configuration up to the reorientation transition temperature (about 0.9 J/k_B), above which it is uniformly magnetized in plane up to the Curie temperature (about 3.8 J/k_B).

The temperature-induced reversed reorientation transition, found experimentally in Ni$_n$/Cu(001) films for $n < 7$, has successfully been described by Hucht and Usadel (1997), who used a perturbative mean-field approach to the model given in equation (1). Using the same parameters, we solved the mean-field equations (20) and (21) and reproduced the reversed reorientation transition without any perturbative treatment. The results for a four-layer film are shown in figures 2 and 3. Although the distribution of the anisotropy parameters is asymmetric, the calculation resulted in identical magnetizations in the first and fourth layers as well as in the second and third layers. Moreover, the angles of the magnetizations in the different layers are almost iden-
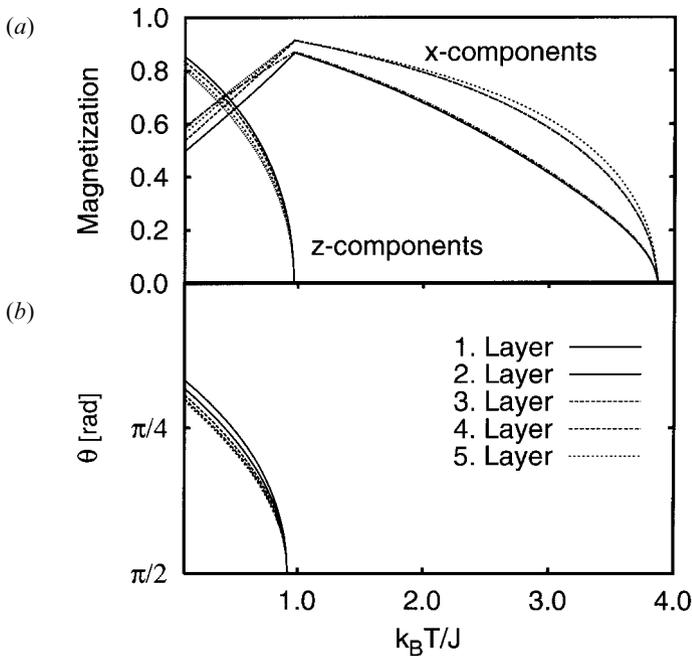
Figure 1. Out-of-plane to in-plane reorientation transition in a five-layer system ($\lambda_1/J = 0.26$, $\lambda_{2,\ldots,5} = 0$, $\omega/J = 0.0056$). The z and the x components of (*a*) the average magnetization and (*b*) the angles of magnetization with respect to the normal of the surface are shown.
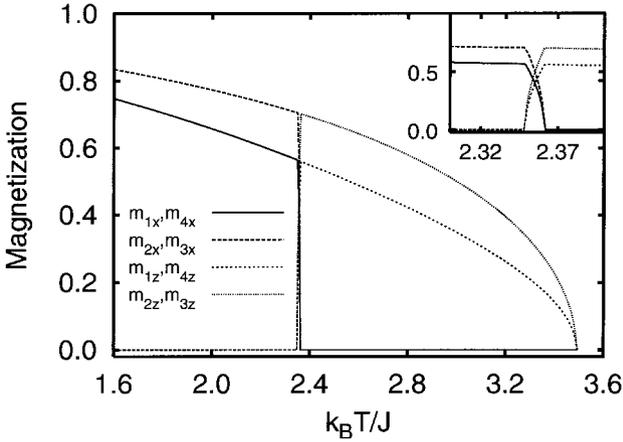
Figure 2. Normal-to-plane and in-plane components of the layer resolved magnetization for a film of four atomic layers exhibiting a reversed reorientation transition. The parameters, representative of Ni were taken from the paper by Hucht and Usadel (1997): $J = 1$, $\lambda_1/J = -3.5 \times 10^{-3}$, $\lambda_i/J = 1.5 \times 10^{-3}(i > 1)$, $\omega/J = 5 \times 10^{-5}$. The inset shows the vicinity of the reorientation transition on an enlarged scale.
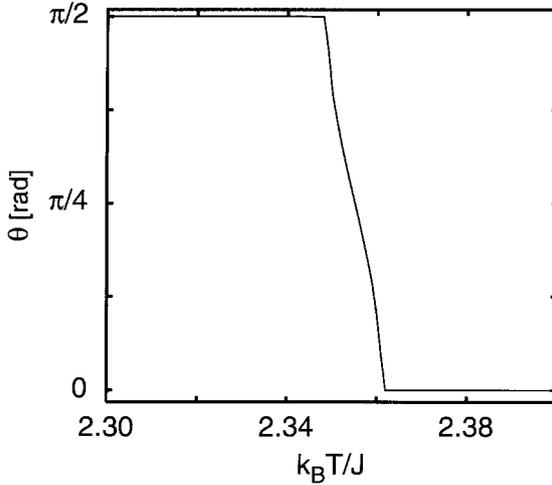
Figure 3. Variation in the angle of average magnetization for the system in figure 2.

tical; in the whole temperature range the largest deviation is smaller than 6×10^{-4} rad.

For a bilayer ($N = 2$) the hyperplanes (7) and (24) reduce to the lines

$$\frac{\lambda_1}{\omega} + \frac{\lambda_2}{\omega} = \frac{3}{2}(A_{11} + A_{12}) \quad \text{and} \quad \frac{\lambda_1}{\omega} + \frac{\lambda_2}{\omega} = \frac{5}{2}(A_{11} + A_{12}), \tag{25}$$

respectively. Apparently, the two lines do not intersect. As a consequence, a reversed reorientation can occur only if the number of layers in the film exceeds two. The same conclusion has been drawn by Hucht and Usadel (1997) using a perturbative treatment of the anisotropy parameters. Nevertheless, it is interesting to note that the

region in the parameter space $\{\lambda_p/\omega\}$ of canted ground states, bounded by the lines defined by equations (9) and (10), always overlaps the region, where the magnetization goes to zero via in-plane orientation. Thus, in this overlapping region an out-of-plane (canted) to in-plane transition, that is reversed reorientation transition can indeed occur. The corresponding parameters ω and $\{\lambda_p\}$, are, however, most likely beyond the physically relevant regime.

For a bilayer, in figure 4 the different regions of phase transitions in the respective parameter space are shown. In regions I and V there is no temperature-driven reorientation transition and the magnetization remains in plane and normal to plane respectively, until T_C is reached. In regions II and III, the magnetization turns into the plane from a canted or a normal-to-plane ground state, respectively. As discussed above, in region IV, a reversed reorientation can occur from a canted ground state to a normal-to-plane direction.

The order of the reorientation transition at finite temperatures has been studied in the literature by the mean-field and Monte Carlo methods. Most workers concluded (Hucht *et al*. 1995, Hucht and Usadel 1996, MacIsaac *et al*. 1996) that the reorientation transition in a monolayer is of first order. For a bilayer, within the mean-field approach, a relatively small range in the vicinity of $\lambda_1 = \lambda_2$ was found, where the system underwent a first order reorientation transition (Hucht and Usadel 1996). In the following, we establish a simple general criterion for the order of the reorientation transition. Suppose that the ground-state magnetization is in plane and its normal-to-plane component appears at the temperature T_{rz}. Since near T_{rz} the z component of the magnetization is small, the exponential function in equation (21) can be expanded up to first order in m_p^z, leading to the homogeneous linear equations

$$\sum_{q=1}^{N} C_{pq}^z m_q^z = 0, \tag{26}$$
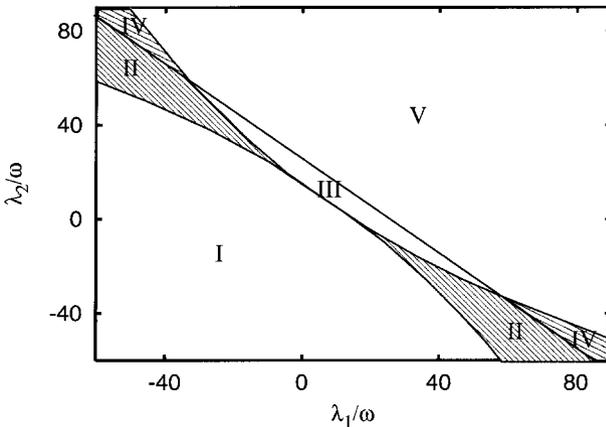
Figure 4. Phase diagram of the magnetic ground states and the reorientation phase transitions for a bilayer, where the magnetic dipole–dipole coupling strength $\omega = 0.01J$: region I, in-plane magnetization up to T_C; region II, canted ground state with reorientation transition to in-plane orientation; region III, normal-to-plane ground state with reorientation transition to in-plane orientation; region IV, canted ground state with reversed reorientation transition; region V, normal-to-plane magnetization up to T_C.

where

$$C_{pq}^z \equiv \delta_{pq} - \beta_{rz} c_{pq}^z \mathcal{Z}_p, \tag{27}$$

$$\mathcal{Z}_p = \frac{2\pi}{Z_p} \int \cos^2(\theta) \exp[\beta_{rz}\lambda_p \cos(\theta)^2] \, J_0[-i\beta_{rz}b_p^x \sin(\theta)] \sin(\theta) \, d\theta \tag{28}$$

and $\beta_{rz} \equiv 1/k_B T_{rz}$. Note that the C_{pq}^z depend only on the in-plane component of the magnetizations m_q^x, which has to satisfy equation (20) for the case when $m_q^z = 0$. Equation (26) has a non-trivial solution only if the determinant of the matrix $C^z = \{C_{pq}^z\}$ is zero. Evidently, this is the condition which determines T_{rz}. Similarly, one can easily find the corresponding equation for T_{rx}, where the in-plane component of the magnetization appears in a normal-to-plane spin configuration,

$$\sum_{q=1}^N C_{pq}^x m_q^x = 0, \tag{29}$$

with

$$C_{pq}^x = \delta_{pq} - \beta_{rx} c_{pq}^x \mathcal{X}_p, \tag{30}$$

$$\mathcal{X}_p = \frac{\pi}{Z_p} \int \sin^3(\theta) \exp[\beta_{rx}\lambda_p \cos^2(\theta)] \{J_0[-i\beta_{rx}b_p^x \sin(\theta)] - J_2[-i\beta_{rx}b_p^x \sin(\theta)]\} \, d\theta \tag{31}$$

and $\beta_{rx} \equiv 1/k_B T_{rx}$. It is easy to show that equations (26) and (29) directly follow from a stability analysis of the mean-field free energy in the vicinity, where the corresponding components of the magnetizations vanish.

The mean-field equations (20) and (21) always have an in-plane and a normal-to-plane solution with magnetizations $m_x^q \neq 0$, $m_z^q = 0$, and $m_z^q \neq 0$, $m_x^q = 0$, respectively. Between T_{rx} and T_{rz}, a canted solution can exist with $m_x^q \neq 0$ and $m_z^q \neq 0$. Of the above three phases, the physical phase is that which has the lowest free energy. In figure 5 (*a*) the free energy of a system possessing a second-order normal-to-plane to in-plane reorientation transition is schematically shown. The ground-state magnetization is perpendicular to the surface of the substrate. At T_{rx} an in-plane component appears in the magnetization. The normal-to-plane component of the
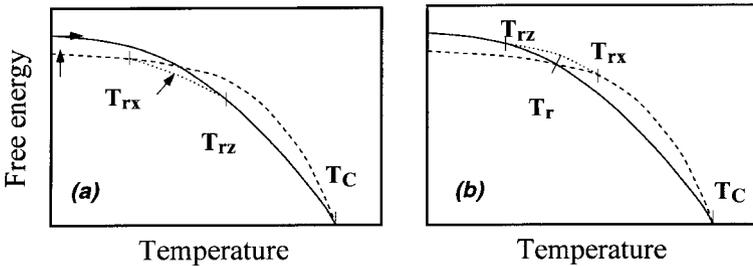
Figure 5. Schematic picture of the free energy in the case of a (*a*) a second-order and (*b*) and a first-order reorientation phase transition. As indicated by arrows, the solid, broken and dotted curves refer to the in-plane, normal-to-plane and canted mean-field solutions respectively.

magnetization vanishes at the temperature $T_{rz}(> T_{rx})$. A similar picture for a first-order transition is shown in figure 5(b). Obviously, one can conclude that, if $T_{rx} < T_{rz}$, a second-order normal-to-plane to in-plane reorientation phase transition occurs whereas, if $T_{rz} < T_{rx}$, the reorientation transition is of first order. In the case of a reversed reorientation, the relation between T_{rx} and T_{rz} is just the opposite to that described above; a second-order transition occurs if $T_{rz} < T_{rx}$, while for $T_{rx} < T_{rz}$ the transition is of first order. At the boundary of the regions, where second-order and first-order phase transitions occur, the two temperatures T_{rx} and T_{rz}, must evidently coincide.

In figure 6, the region of first-order reorientations (III F) and that of second-order reorientations (III S) are shown in the phase diagram for a bilayer. Note that figure 6 in fact represents figure 4 on an enlarged scale for the parameters $0 < \lambda_{1,2}/\omega < 18$. This picture is consistent with the observation of Hucht and Usadel (1996) for the range of the first-order reorientation phase transitions, as they performed investigations very close to the critical point only. In that case, by keeping $\lambda_1 + \lambda_2$ fixed, figure 6 implies a very narrow range for the first-order transitions.

The phase diagram of the trilayer case ($N = 3$) is shown in figure 7. Apparently, the same regimes exist as in the case of a bilayer. The region of first-order reorientation transition forms now a 'sack', touching the plane defined by equation (7) at the critical point given by equation (14). The 'sack' is covered by the plane separating the area where normal-to-plane to in-plane reorientation occur and the area, where the magnetization remains normal to plane up to the Curie temperature (see equation (24)). The regime of reversed reorientation transitions, part of the region of second-order transitions, is, however, out of the segment of the parameter space depicted in figure 7.

Numerical calculations using different magnetic dipole–dipole coupling strengths ω (see, in particular, figure 6) yield almost the same boundaries in the $\{\lambda_p/\omega\}$ para-
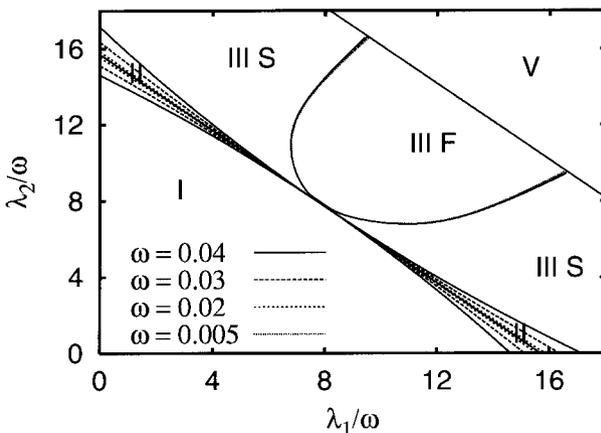
Figure 6. Phase diagram of reorientation transitions for a bilayer ($N = 2$). Regions I, II, III and V denote the same regions as in figure 4; regime III, however, is partitioned into regions referring to first-order (III F) and second-order (III S) normal reorientation phase transitions. The corresponding boundary lines are shown for different values of the magnetic dipole–dipole interaction strength ω, measured in units of J.
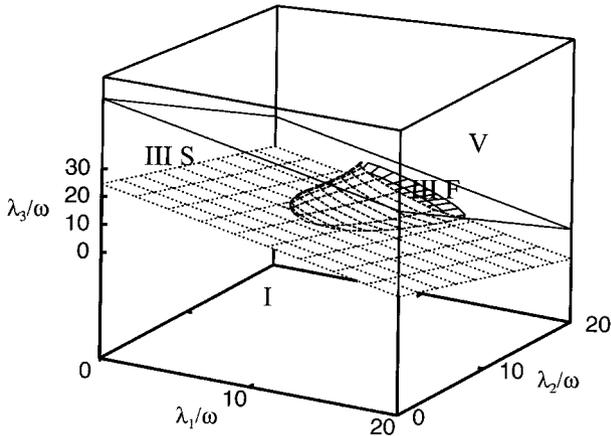
Figure 7. Mean-field phase diagram of reorientation transitions for a trilayer ($N = 3$): region I, in-plane magnetization up to T_C; region III S, second-order normal-to-plane to in-plane reorientation; region III F, first-order normal-to-plane to in-plane reorientation; region V, normal-to-plane magnetization up to T_C.

meter space of the phase diagrams for both the bilayer and the trilayer cases. The only exception is the region of the canted ground states, which rapidly opens up with increasing ω. The established *universality* of the phase boundaries nicely confirms that the reorientation phase transitions, as long as ω becomes comparable with J, are a consequence of the competition between the uniaxial anisotropy and the magnetic dipole–dipole interaction.

§4. Conclusions

In the present paper we provided a full account of the ground states and of the finite-temperature behaviour of a ferromagnetic film with a finite number of layers, as described by the classical vector spin Hamiltonian (1), including exchange coupling interaction, uniaxial magnetocrystalline anisotropies and magnetic dipole–dipole interaction. We derived explicit expressions for the boundaries of the regions related to normal-to-plane, canted and in-plane ground states in the corresponding parameter space. We concluded that within the model, defined by equation (1), canted ground states are ultimately connected to non-collinear spin configurations. In addition, as established so far for monolayers only (Hucht and Usadel 1996), for any thickness of the film we proved the existence of a critical point, where the ground-state energy of the system is independent of the uniform orientation of the magnetization.

We also investigated intensively the finite-temperature behaviour of the system in terms of a mean-field theory. By using a high temperature expansion technique, we showed that the Curie temperature of a ferromagnetic film can be calculated by solving an eigenvalue problem, which, for the case of a bulk system and by neglecting anisotropy effects, leads to the well-known expression for T_C. The main part of the present study has been devoted to the reorientation phase transitions, which play a central role for applications of thin-film and multilayer systems as high-storage magnetic recording devices. Both the normal-to-plane to in-plane and the in-plane to normal-to-plane (reversed) temperature-induced reorientation transitions have

been discussed and the corresponding regions in parameter space have been explicitly determined. In accordance with previous studies (Hucht and Usadel 1997), we showed that, for physically relevant parameters, reversed reorientation can occur only for films containing three or more atomic layers. By investigating the order of reorientation phase transitions, we found well-defined conditions for the first- and the second-order phase transitions and presented the corresponding regions for bilayers and trilayers in the respective parameter spaces.

In conclusion, we have shown that a mean-field treatment of a classical vector spin model recovers most of the important phenomena observed in magnetic thin film measurements at finite temperatures. Without any doubt, owing to the lack of mean field theories for low-dimensional systems, some of them have to be refined by using more sophisticated methods of statistical physics (see § 1). In particular, for very thin films (monolayers), the mean-field theory predicts a T_C much higher than the random-phase approximation. However, by rescaling the temperature, the orientations of the magnetization become fairly similar in both approaches (Fröbrich *et al.* 2000a,b). As far as the first principles attempts (Szunyogh *et al.* 1995, 1997b, Szunyogh and Udvardi 1998, 1999, Uiberacker *et al.* 1999, Pajda *et al.* 2000) are concerned, which are currently able to calculate realistic parameters for a model such as equation (1), the technique presented and applied here provides a simple and quick tool to study the finite temperature behaviour of thin magnetic films. As the measurements are performed at finite temperatures, while first principles calculations usually refer to the ground state, such a procedure would improve the predictive power of *ab-initio* theories. It should also be mentioned that first attempts at an *ab-initio* type of description of thin magnetic films at finite temperatures, that is taking into account the coupling of the itinerant nature of the electrons and the spin degree of freedom, are currently in progress (Razee *et al.* 2001).

APPENDIX A
DERIVATION OF THE CURIE TEMPERATURE

In the high-temperature limit ($\beta \to 0$, $\beta b_p^{x(z)} \to 0$) the partition function as given by equation (17) can be written up to the first order of the magnetization as

$$Z_p = 2\pi \int_{-1}^{1} (1 + \beta b_p^z z) \exp(\beta\lambda_p z^2)\, dz = 2\pi \int_{-1}^{1} \exp(\beta\lambda_p z^2)\, dz. \qquad (A\,1)$$

Similarly, for the magnetization in equation (21) the following approach can be used:

$$m_p^z = \frac{2\pi}{Z_p} \int_{-1}^{1} z[1 + \beta(b_p^z + H)z] \exp(\beta\lambda_p z^2) \, \mathrm{d}z$$

$$= \frac{1}{\lambda_p}(b_p^z + H)\left(\frac{\exp(\beta\lambda_p)}{\int_{-1}^{1} \exp(\beta\lambda_p z^2) \, \mathrm{d}z} - \frac{1}{2}\right), \tag{A 2}$$

where an external magnetic field H has been added to the Hamiltonian in equation (16). By substituting the expansion

$$\frac{\exp(\beta\lambda_p)}{\int_{-1}^{1} \exp(\beta\lambda_p z^2) \, \mathrm{d}z} = \tfrac{1}{2} + \tfrac{1}{3}\beta\lambda_p + \tfrac{4}{45}(\beta\lambda_p)^2 + \mathcal{O}(\lambda_p^2) \tag{A 3}$$

into equation (A 3), it follows that

$$m_p^z = \beta(b_p^z + H)(\tfrac{1}{3} + \tfrac{4}{45}\beta\lambda_p). \tag{A 4}$$

Requiring non-vanishing magnetization at zero external field results in the following eigenvalue problem

$$\sum_{q=1}^{N} c_{pq}^z (1 + \tfrac{4}{15}\beta\lambda_p) m_q^z = 3k_{\mathrm{B}} T m_p^z. \tag{A 5}$$

Let T_z denote the highest value of T, for which equation (A 5) is satisfied, that above which no spontaneous normal-to-plane magnetization can exist. A similar procedure can be applied in order to determine T_x, that is the temperature at which the in-plane magnetization vanishes. Quite obviously, by neglecting anisotropy effects, for a bulk system the Curie temperature $T_{\mathrm{C}} = T_x = T_z$ is given by the well-known formula

$$T_{\mathrm{C}} = \frac{nJ}{3k_{\mathrm{B}}}, \tag{A 6}$$

where n denotes the number of nearest neighbours in the bulk.

With the exception of very open surfaces such as the bcc (111) surface (see table 1), the magnetic dipole–dipole coupling constants A_{pq} fall off exponentially with increasing distance between layer p and layer q. Therefore, as an approximation we neglect all A_{pq} for $|p - q| > 1$, which, by recalling the nearest-neighbour approximation for the exchange coupling, implies that the matrix formed by the elements c_{pq}^z is tridiagonal. The non-vanishing elements are then written as

$$c_{pp}^z = n_{11}J - A_{11}\omega, c_{p,p-1}^z = c_{p-1,p}^z = n_{12}J - A_{12}\omega. \tag{A 7}$$

Setting $\lambda_p = 0$, the solution of the eigenvalue problem (A 5) yields

$$T_z^{(0)} = \frac{1}{k_{\mathrm{B}}}\left[n_{11}J - A_{11}\omega + 2(n_{12}J - A_{12}\omega)\cos\left(\frac{\pi}{N+1}\right)\right], \tag{A 8}$$

with the components of the corresponding normalized eigenvector $u_p = [2/(N+1)]^{1/2} \sin[p\pi/(N+1)]$. Substituting $T_z^{(0)}$ into equation (A 5) and using first-order perturbation theory with respect to λ_p, one obtains equation (23) for T_z. Again, a similar procedure applies for deriving T_x in equation (22).

References

Abramowitz, M., and Stegun, I. A. (editors), 1972, *Handbook of Mathematical Functions with Formulas, Graphs and Mathematical Tables* (New York: Dover Publications).

Allenspach, R., 1994, *J. Magn. magn. Mater.*, **129**, 160.

Allenspach, R., Stampanoni, M., and Bischof, A., 1990, *Phys. Rev. Lett.,* **65**, 3344.

Berger, A., and Hopster, H., 1996, *Phys. Rev. Lett.,* **76**, 519.

Bruno, P., 1991, *Phys. Rev. B*, **43**, 6015.

Chui, S. T., 1995, *Phys. Rev. Lett.,* **74**, 3896.

Farle, M., Platow, W., Anisimov, A. N., Poulopoulos, P., and Baberschke, K., 1997, *Phys. Rev. B*, **56**, 5100.

Fröbrich, P., Jensen, P. J., and Kuntz, P. J., 2000a, *Eur. Phys. J.* B, **13**, 477.

Fröbrich, P., Jensen, P. J., Kuntz, P. J., and Ecker, A., 2000b, *Eur. Phys. J.* B, **18**, 579.

Garreau, G., Beaurepaire, E., Ounadjela, K., and Farle, M., 1996, *Phys. Rev. B*, **53**, 1083.

Gradmann, U., 1986, *J. Magn. magn. Mater.*, **54–57**, 733.

Gubiotti, G., Carlotti, G., Socino, G., D'Orazio, F., Lucari, F., Bernardini, R., and Crescenzi, M. D., 1997, *Phys. Rev. B*, **56**, 11 073.

Herrmann, T., Potthoff, M., and Nolting, W., 1998, *Phys. Rev. B*, **58**, 831.

Hjortstam, O., Baberschke, K., Wills, J. M., Johansson, B., and Eriksson, O., 1997, *Phys. Rev. B*, **56**, R4398.

Hu, L., Li, H., and Tao, R., 1999, *Phys. Lett.* A, **254**, 361.

Hucht, A., Moschel, A., and Usadel, K. D., 1995, *J. Magn. magn. Mater.*, **148**, 32.

Hucht, A., and Usadel, K. D., 1996, *J. Magn. magn. Mater.*, **156**, 423; 1997, *Phys. Rev. B*, **55**, 12 309; 1999a, *J. Magn. magn. Mater.*, **198–199**, 491; 1999b, *ibid.,* **203**, 88; 2000, *Phil. Mag.* B, **80**, 275.

Jensen, P. J., and Bennemann, K. H., 1998, *Solid St. Commun.,* **105**, 577.

Jensen, P. J., Bennemann, K. H., Baberschke, K., Poulopoulos, P., and Farle, M., 2000, *J. appl. Phys.*, **87**, 6692.

Li, D., Freitag, M., Pearson, J., Qiu, Z. Q., and Bader, S. D., 1994, *Phys. Rev. Lett.*, **72**, 3112.

MacIsaac, A. B., Whitehead, J. P., De'Bell, K., and Poole, P. H., 1996, *Phys. Rev. Lett.*, **77**, 739.

Mills, D. L., 1989, *Phys. Rev. B*, **39**, 12 306.

Moschel, A., and Usadel, K. D., 1994, *Phys. Rev. B*, **49**, 12 868; 1995, *ibid.,* **51**, 16 111.

Pajda, M., Kudrnovský, J., Turek, I., Drchal, V., and Bruno, P., 2000, *Phys. Rev. Lett.,* **85**, 5424.

Pappas, D. P., Brundle, C. R., and Hopster, H., 1992, *Phys. Rev. B*, **45**, 8169.

Pappas, D. P., Kämper, K. P., and Hopster, H., 1990, *Phys. Rev. Lett.,* **64**, 3179.

Pescia, D., and Pokrovsky, V. L., 1990, *Phys. Rev. Lett.,* **65**, 2599.

Razee, S. S. A., Staunton, J. B., Szunyogh, L., Újfalussy, B., and Györffy, B. L., 2001 (to be published).

Serena, P. A., Garcia, N., and Levanyuk, A., 1993, *Phys. Rev. B*, **47**, 5027.

Szunyogh, L., and Udvardi, L., 1998, *Phil. Mag.* B, **78**, 617; 1999, *J. Magn. magn. Mater.*, **198–199**, 537.

Szunyogh, L., Újfalussy, B., Blaas, C., Pustogowa, U., Sommers, C., and Weinberger, P., 1997a, *Phys. Rev. B*, **56**, 14 036.

Szunyogh, L., Újfalussy, B., and Weinberger, P., 1995, *Phys. Rev. B*, **51**, 9552; 1997b, *ibid.,* **55**, 3765.

Taylor, M. B., and Györffy, B. L., 1993, *J. Phys.: condens. Matter*, **5**, 4527.

Timm, C., and Jensen, P. J., 2000, *Phys. Rev. B*, **62**, 5634.

Udvardi, L., Király, R., Szunyogh, L., Denat, F., Taylor, M. B., Györffy, B. L., Újfalussy, B., and Uiberacker, C., 1998, *J. Magn. magn. Mater.,* **183**, 283.

Uiberacker, C., Zabloudil, J., Weinberger, P., Szunyogh, L., and Sommers, C., 1999, *Phys. Rev. Lett.,* **82**, 1289.

Újfalussy, B., Szunyogh, L., and Weinberger, P., 1996, *Phys. Rev. B*, **54**, 9883.

Weinberger, P., 1997, *Phil. Mag.* B, **75**, 509.

Weinberger, P., and Szunyogh, L., 2000, *Comput. Mater. Sci.,* **17**, 414.

Zabloudil, J., Szunyogh, L., Pustogowa, U., Uiberacker, C., and Weinberger, P., 1998, *Phys. Rev. B*, **58**, 6316.